Max-Planck-Institut
für Mathematik
in den Naturwissenschaften
Leipzig

Generalized and partial synchronization of coupled neural networks

by

Frank Pasemann and Thomas Wennekers

Preprint no.: 48 1999

Generalized and Partial Synchronization of Coupled Neural Networks

Frank Pasemann and Thomas Wennekers
Max-Planck-Institute for Mathematics in the Sciences
Inselstr. 22-26, D-04103 Leipzig, Germany
Email: (pasemann,wennekers)@mis.mpg.de

Abstract

Synchronization of neural signals has been proposed as a temporal coding scheme representing cooperated computation in distributed cortical networks. Previous theoretical studies in that direction mainly focused on the synchronization of coupled oscillatory subsystems and neglected more complex dynamical modes, that already exist on the single-unit level. In the present work we study the parameterized time-discrete dynamics of two coupled recurrent networks of graded neurons. Conditions for the existence of partially synchronized dynamics of these systems are derived, referring to a situation where only subsets of neurons in each sub-network are synchronous. The coupled networks can have different architectures and even a different number of neurons. Periodic as well as quasiperiodic and chaotic attractors constrained to a manifold M of synchronized components are observed. Examples are discussed for coupled 3-neuron networks having different architectures, and for coupled 2-neuron and 3-neuron networks. Partial synchronization of different degrees is demonstrated by numerical results for selected sets of parameters. In conclusion, the results show that synchronization phenomena far beyond completely synchronized oscillations can occur even in simple coupled networks. The type of the synchronization depends in an intricate way on stimuli, history and connectivity as well as other parameters of the network. Specific inputs can further switch between different operational modes in a complex way, suggesting a similarly rich spatio-temporal behavior in real neural systems.

1 Introduction

Synchronization of neural activity in biological brains has been observed in different species, areas and under various physiological conditions (cf. [7, 14, 20, 29, 32, 44, 45]. Most attention was given to the experimental evidence that coherent firing of spatially separate neurons appears as a response to specific external stimuli, in particular in response to extended object borders that may cover more than the classical receptive fields of the stimulated cells. The observation of synchrony between firing activity at distant sites along continuous edges lead to the famous "binding hypothesis" which states that the synchronization of neural activity serves as a fundamental temporal mechanism for binding spatially distributed features into a coherent object representation (cf. e.g. [14, 15, 44]). In this context conceptual discussions and biologically motivated models were mainly based on the synchronization of oscillatory dynamics in high-dimensional systems (cf. e.g. [9, 17, 22, 38, 39, 51, 56], and reviews in [18, 53]).

Interestingly, although a matter of intensive research for the last 10 years there is still no common agreement about the precise origin of cortical gamma-oscillations. Several alternatives have been proposed:

1. Many theoretical studies assume that collective oscillations arise from coupled networks of intrinsically periodically firing excitatory cells that mutually align their spikes in time (reviews in [18, 53]). Inhibitory interneurons in this interpretation mainly regulate the firing frequency or are neglected at all.

2. In strong contrast Buzsàki and Chrobak [7, 51] suggested that the oscillations arise from networks of *inhibitory* cells that synchronize by themselves and co-operatively entrain large populations of principal/pyramidal cells. Individual principal cells in their scenario may fire at low rates and non-rhythmic. Their firing times, however, are correlated with the membrane oscillations induced by the inhibitory subnetwork.

3. A third alternative is that gamma-oscillations are not characterized by mutually synchronizing ensembles of already periodically firing individual cells (either excitatory or inhibitory), but that the rhythm is a collective effect due to mass action between two pools of excitatory and inhibitory cells [45, 54, 56]. Cells in both pools can reveal broad firing frequency distributions and only weak spike synchrony [54].

4. In addition, although it is commonly believed that gamma-oscillations are cortex-intrinsically generated and synchronized by lateral or cortico-cortical fibres, some authors suggested that synchrony (either oscillatory or non-oscillatory) may at least in part be input driven [19].

Since there is experimental evidence for all these alternatives it is likely that different mechanisms participate in the generation and synchronization of gamma-oscillations in different brain structures, areas or even within the same area.

Most interestingly in the context of the present paper is, that the different alternatives can and have all been simulated in computational neural network studies employing an architecture of internally as well as mutually connected pools of excitatory and inhibitory neurons (e.g. [17, 18, 28, 46, 51, 53, 54, 56]). Although the cited simulation studies are not perfectly comparable in their modeling details and physiological realism they nonetheless show that in such excitatory-inhibitory networks case 1 above corresponds to neglectable inhibition [11, 18]. In contrast, case 2 occurs if interneurons inhibit themselves sufficiently strongly and excitation is relatively weak or missing at all (e.g. [46, 51]). Case 3 requires approximately balanced excitation and inhibition above some critical level and a certain amount of disorder in the network, say, in form of randomly chosen synaptic weights or strong temporal input noise [54, 56]. Of course, also stimulus locked input driven correlations (case 4) can be induced in such networks (see e.g. [28]).

This means: depending on the parameters chosen, essentially the same network can reveal completely different dynamics; either the excitatory subnetwork synchronizes, or the inhibitory one, or both interact and lead to mass oscillations. In response to appropriate (i.e. correlated) input the level of synchronization within the network may further depend more on the input drive or the recurrent feedback.

Previous research on cortical synchronization phenomena of this kind has focused almost exclusively on coupled oscillatory systems. Only a few model studies consider synchronization of coupled systems in other dynamical modes, for example, stationary stochastic firing states or chaotic dynamics [23, 28, 48].

Furthermore, many studies seem to be guided by the idea of what we call "complete synchronization", i.e. they attempt a collectively synchronized dynamical state, where all cells in the network fire synchronously in every oscillation period. The physiological unrealism of this "tight-binding" situation (cf. [53]) is sometimes in part counteracted by introducing noise into the system. This lets simulated observables (membrane potentials, spike trains, correlation functions, etc.) look more like their real physiological counterparts, but it does not change the principal concept of tightly synchronized oscillations.

On the other hand it is known, that already single neurons due to a variety of intrinsical non-linearities can reveal complex dynamics in response to current injection or various transmitter substances [21, 24, 39]. Evidence for chaotic dynamics has also been found on the network level, expressed, for instance, in mass signals like local field potentials or the EEG [13, 45].

The coupling of strongly nonlinear chaotic subsystems, however, has only been addressed in neurobiological contexts in a few example studies [23, 45]. Complete synchronization as for coupled oscillations has been demonstrated in chaotic sys-

tems [43, 36, 37], but a multitude of further interesting dynamical phenomena seems to exist, including weaker forms of "partial" or "generalized" synchronization (for definitions see section 2), hysteresis between co-existing chaotic and nonchaotic attractors, hyperchaos, and more (e.g. [12, 25, 40]).

Hence, it seems that in restricting attention to tightly coupled oscillations only, brain theory appears unaware of the rich phenomenology of coupled nonlinear subsystems. The following investigations therefore may serve as an inspiration for the modelling of various computational and cognitive processes. Following a modular approach to neural systems [33], we ask, how the synchronized activity of subsets of module neurons depends on the module interactions as well as on the module inputs.

On this background we study the parameterized time-discrete dynamics of two coupled neural networks with recurrent connectivity. These small subsystems - called *neuromodules* because they are considered as basic building blocks for larger neural networks - are described as low-dimensional dynamical systems with nonlinearities introduced by the sigmoidal transfer functions of standard additive neurons. As parameters we will consider bias terms and/or stationary inputs, the synaptic weights between module neurons, and the coupling strength between neurons of different modules.

Outline of the paper is as follows: The next section sets up the formalism for coupled neuromodules and gives definitions for their partial as well as for their generalized synchronization. Complete synchronization is of course a special case of partial synchronization. Definitions allow to describe the behavior of coupled identical as well as non-identical systems, which can even be composed of subsystems having different internal connectivity structures and dimensionality. General conditions for the existence of partially synchronized dynamics of coupled neuromodules are derived. These conditions show that asymmetric recurrent coupling of modules, which have different numbers of neurons or different architectures, can "compensate" these differences to achieve partial synchronization even between *different* coupled subsystems.

The partially synchronized dynamics of two modules can be stable or unstable, where stability is understood in the sense that small perturbations of synchronized states will not desynchronize the system. Analytical treatments of stable synchronization often use linear (diffusive) coupling schemes (e.g. [30]); but in the neural network context we canonically have to deal with the nonlinear coupling of subsystems. This makes analytical statements about the stability conditions for the synchronous dynamics much more difficult to achieve. We will discuss stability properties of a synchronous dynamics along well established lines [4, 49]: A *manifold of synchronized components* M is introduced together with its *synchronization* and *transversal Lyapunov exponents*. Partially synchronized chaos will be characterized by at least one positive synchronization exponent; unstable synchronized dynamics by at least one positive transversal exponent. Thus, unstable partially synchronized chaos will always be associated with hyperchaotic

systems, i.e. with systems having at least two positive Lyapunov exponents [42].

In sections 3 and 4 we present numerical examples for the different kinds of synchronization. First we couple a 3-neuron ring network with a bi-directional chain of three neurons. The dynamical features of the isolated systems are quite different – besides fixed point attractors 3-rings can have period-2, -3 and period-6 attractors [34], whereas 3-chains can have p-periodic attractors for all p, and quasi-periodic and chaotic attractors as well [33]. For this coupled system partial synchronization of degree 1 (only two neurons are synchronized) and of degree 2 (only two pairs of neurons are synchronized), as well as generalized synchronous dynamics are demonstrated. Complete synchronization for this setup was reported in [37]. Section 4 presents the dynamics of a chaotic 2-neuron module coupled to a bi-directional chain of three neurons. The 2-neuron module can be understood in terms of the Wilson-Cowan model of excitatory and inhibitory neuron interaction [55], and its dynamical behavior is well known for large parameter domains [5, 8, 33, 50]. Example dynamics for coupling schemes leading to stable as well as unstable partial synchronization of degree 1 and 2 are given for this case.

Section 5 gives a summary of results and a general discussion of synchronization effects in neural networks.

2 Coupled neuromodules

We are considering neuromodules as discrete parameterized dynamical systems on an n-dimensional activity phase space $\mathbf{R}^n$ given by the map

$$a_i(t+1) = \theta_i + \sum_{j=1}^{n} w_{ij}\,\sigma(a_j(t)) \;, \quad i = 1, \ldots, n \;, \tag{1}$$

where $a_i \in \mathbf{R}^n$ denotes the activity of the i-th neuron, and $\theta_i = \overline{\theta}_i + I_i$ denotes the sum of its fixed bias term $\overline{\theta}_i$ and its stationary external input I_i, respectively. The output $o_i = \sigma(a_i)$ of a unit is given by the sigmoidal transfer function $\sigma(a) := (1 + e^{-a})^{-1}$, $a \in \mathbf{R}$, and w_{ij} denotes the synaptic weight from unit j to unit i. A neuromodule having a parameter set $\rho = (\theta, w)$ for which the dynamics (1) has at least one chaotic attractor will be called a *chaotic neuromodule*.

Suppose A and B denote two neuromodules having n and m neurons, respectively. Correspondingly, their architectures will be described by an $(n \times n)$-matrix w^A and by an $(m \times m)$-matrix w^B. Connections going from module B to module A are comprised in an $(n \times m)$ coupling matrix w^{AB}. Correspondingly, connections from module A to module B are given as an $(m \times n)$ coupling matrix w^{BA}. Thus, the architecture of the coupled system is given by a matrix w of the form

$$w = \begin{pmatrix} w^A & w^{AB} \\ w^{BA} & w^B \end{pmatrix} \;, \tag{2}$$

and the pair (w^{AB}, w^{BA}) of matrices will be called the *coupling structure*. A coupling structure (w^{AB}, w^{BA}) will be called *symmetric*, iff $w^{AB} = w^{BA}$, and a *one-way coupling*, iff $w^{AB} = 0$ or $w^{BA} = 0$ (but not both) .

For simplicity we would like to have modules of the same dimension. Suppose $n > m$; then we will add $(n-m)$ isolated neurons to the m neurons of module B, so that formally B has also n neurons. Thus, in the following the weight matrix (2) will be considered as a $(2n \times 2n)$-matrix.

The neural activities of module A and B will be denoted a_i, b_i, $i = 1, ...n$, respectively. The activity phase space of the coupled system is then $2n$-dimensional, and its discrete parameterized dynamics will be denoted by $F_\rho : \mathbf{R}^{2n} \to \mathbf{R}^{2n}$. Here $\rho := (\rho^A,\ \rho^B,\ w^{AB},\ w^{BA})$ denotes a set of parameters for the coupled system and $\rho^A := (\theta^A,\ w^A)$ is the parameter set of module A. Furthermore, if $m < n$ the activities of the $(n-m)$ isolated neurons added to module B will be constant, and we will set $b_i = 0$ for $i = m+1, \ldots, n$. Thus, the dynamics F_ρ will be given in the form

$$a_i(t+1) = \theta_i^A + \sum_{j=1}^{n} w_{ij}^A\, \sigma(a_j(t)) + \sum_{j=1}^{n} w_{ij}^{AB}\, \sigma(b_j(t))\,, \tag{3}$$

$$b_i(t+1) = \theta_i^B + \sum_{j=1}^{n} w_{ij}^B\, \sigma(b_j(t)) + \sum_{j=1}^{n} w_{ij}^{BA}\, \sigma(a_j(t))\,. \tag{4}$$

We are now mainly interested in the case where a subset of module neurons have identical activities during a dynamical process. But sometimes it is interesting to consider situations, where the coupling of two systems results in a dynamics which is constrained to a d-dimensional manifold, $d < 2n$, without being synchronous [1]. This means that the coupling induces some functional relation between the states of the two modules. More precisely, we will use the following

Definition 1 *Suppose there exist units i_m, $m = 1, \ldots, k$, $k \leq n$, a homeomorphism $\Phi : \mathbf{R}^k \to \mathbf{R}^k$, and a subset $D \subset \mathbf{R}^{2n}$, such that $(a_0, b_0) \in D$ implies*

$$\lim_{t\to\infty} \mid \Phi(a_{i_m}(t; a_0)) - b_{i_m}(t; b_0) \mid = 0\ , \quad m = 1, \ldots, k\ , \tag{5}$$

where $(a(t; a_0), b(t; b_0))$ denotes the orbit under F_ρ through the initial condition $(a_0, b_0) \in \mathbf{R}^{2n}$. Then this process is called a generalized partial synchronization of degree k *of modules A and B.*

Definition 2 *A generalized partial synchronization is called* global, *iff $D \equiv \mathbf{R}^{2n}$, and* local, *iff $D \subset \mathbf{R}^{2n}$ is a proper subset. If k is maximal, i.e. $k = n$, then it is called a* generalized synchronization. *If $\Phi = id$ and $k \leq n$, then a generalized partial synchronization is called a* partial synchronization. *If $\Phi = id$ and $k = n$, then it is called a* complete synchronization.

Thus, complete synchronization is a special case of a generalized synchronization. Furthermore, a partial synchronization can be at the same time also a generalized partial synchronization; i.e. the homeomorphism Φ acts as the identity only on some but not all components. An example for this situation will be given in section 3.3. If the condition (5) is satisfied for $\Phi = id$, we will say that modules A and B synchronize on a subset of k neurons. From definition 1 it follows that only modules with the same number n of non-isolated neurons can have a nontrivial completely synchronized dynamics.

Although defined here for just two coupled modules comprising time-discrete neurons with sigmoid output functions, we should note, that complete, generalized, and partial synchronization can also occur in networks of more realistic "spiking" neurons.

Complete synchronization can be characterized by perfectly synchronous firing of all cells in the network. This occurs, for example, in networks of identical and excitatorily connected integrate-and fire cells. Mirollo and Strogatz have given a rigorous analytical proof that a large class of such networks reaches complete synchronization in finite time for almost all initial conditions [31].

Generalized synchronization can appear, when the cells in the network are not identical. In reference [46] Traub et al. have shown that different input currents into excitatory cells within a network of excitatory and inhibitory neurons can lead to collective oscillations in the gamma-range, where the excitatory cells reveal systematic phase-shifts in firing times relative to this collective oscillation; less input current usually delays firing. Therefore, individual excitatory cells are not completely synchronized, but their firing times are related by some static functional relationship, that is, they are synchronized in the generalized sense. Of course, also scattering synaptic strengths, transmission delays or other parameters varying across neurons may induce such systematic deviations from perfect synchrony.

Some kind of partial synchronization appeared, for example, in a study by Pinsky and Rinzel [39]. Here, 100 excitatorily connected two-compartment neurons were simulated, each containing fast currents responsible for sodium spiking on a soma-like compartment and slower calcium and calcium-mediated currents on a dendrite-like compartment. Formally, each cell was described as an 8-dimensional dynamical system. Isolated neurons, in response to input currents, revealed different firing modes; regular spiking at moderate and high input currents, different kinds of bursting at low inputs, and apparently chaotic dynamics in between. When cells were coupled (via AMPA and NMDA synapses), Pinsky and Rinzel observed a collective dynamical mode of burst-synchronization, where all cells fired regular high-frequency bursts of spikes on a long time-scale (roughly a few hundred milliseconds), but the fast spikes within bursts where not synchronized. Although the synchronization of the slow dynamical variables was not perfect, this can be viewed as partial synchronization, where the slow burst-mediating variables become (up to small deviations) restricted to a low-dimensional mani-

fold, but the fast variables responsible for sodium spiking remain asynchronous (presumably chaotic, although this is not perfectly clear from [39]).

To analyse a partially synchronized dynamics it is convenient to introduce new coordinates as follows:

$$\xi_i := \frac{1}{\sqrt{2}}(a_i + b_i) \quad , \quad \eta_i := \frac{1}{\sqrt{2}}(a_i - b_i) \; , \quad i = 1, \ldots, n \; . \tag{6}$$

In terms of these (ξ, η)-coordinates the dynamics $\tilde{F}_\rho$ of the coupled system reads

$$\begin{aligned} \xi_i(t+1) = \frac{1}{\sqrt{2}} \cdot (\theta_i^A + \theta_i^B) \quad &+ \quad \frac{1}{\sqrt{2}} \sum_{j=1}^{n} (w_{ij}^A + w_{ij}^{BA}) \cdot g^+(\xi_j(t), \eta_j(t)) \\ &+ \quad \frac{1}{\sqrt{2}} \sum_{j=1}^{n} (w_{ij}^B + w_{ij}^{AB}) \cdot g^-(\xi_j(t), \eta_j(t)) \; , \end{aligned} \tag{7}$$

$$\begin{aligned} \eta_i(t+1) = \frac{1}{\sqrt{2}} \cdot (\theta_i^A - \theta_i^B) \quad &+ \quad \frac{1}{\sqrt{2}} \sum_{j=1}^{n} (w_{ij}^A - w_{ij}^{BA}) \cdot g^+(\xi_j(t), \eta_j(t)) \\ &- \quad \frac{1}{\sqrt{2}} \sum_{j=1}^{n} (w_{ij}^B - w_{ij}^{AB}) \cdot g^-(\xi_j(t), \eta_j(t))) \; , \end{aligned} \tag{8}$$

where $i = 1, \ldots, n$, and the functions $g^\pm$ are defined by

$$g^\pm(x, y) := \sigma\left(\frac{1}{\sqrt{2}}\,(x \pm y)\right) \; , \quad x, \; y \in \mathbf{R} \; .$$

A partially synchronized orbit $(\xi(t), \eta(t)), \; t = 0, 1, 2, \ldots$, of the coupled system satisfies $\eta_i(t) = 0$ for all $t = 0, 1, 2, \ldots$, and $i = 1, \ldots, k, \; k \leq n$. The $s_i := \frac{1}{\sqrt{2}}\xi_i = a_i = b_i$ are called *synchronized components*. Using the (ξ, η)-coordinates the following statements can be easily verified.

Lemma 1 *Let $I_s = \{i_1, \ldots, i_k\}$ denote an index set with $k \leq n$. Assume that the parameter sets ρ^A, ρ^B and the coupling structure (w^{AB}, w^{BA}) of the modules A and B satisfy the following conditions for $m = 1, \ldots, k$:*

$$\theta_{i_m}^A = \theta_{i_m}^B \; , \quad (w_{i_m j}^A - w_{i_m j}^{BA}) = (w_{i_m j}^B - w_{i_m j}^{AB}) \; , \quad j \in I_s \tag{9}$$

$$w_{i_m j}^A = w_{i_m j}^{BA} \; , \; w_{i_m j}^B = w_{i_m j}^{AB} \; , \quad j \in \{1, \ldots, n\} \setminus I_s \; . \tag{10}$$

Then there exists a partially synchronized dynamics constrained to a (2n-k)-dimensional F_ρ-invariant manifold

$$M(k) := \{(a, b) \in \mathbf{R}^{2n} \mid b_{i_m} = a_{i_m}, \; m = 1, \ldots, k\} \; . \tag{11}$$

Proof: It suffices to show that if the synchronization conditions (9) and (10) are satisfied, then every orbit of F_ρ through a state partially synchronized on neurons $i_1, \ldots, i_k$ stays partially synchronized on those neurons for all times. This follows

by insertion of (9) and (10) into (8) and the observation that $g^+(x,0) = g^-(x,0)$. If for some time $t = t_0$ we have $\eta_{i_m}(t_0) = a_{i_m}(t_0) - b_{i_m}(t_0) = 0$ for $m = 1, \ldots, k$, then, with respect to the dynamics $\tilde{F}_\rho$ one immediately gets $\eta_{i_m}(t) = 0$, $m = 1, \ldots, k$ for all $t > t_0$ from (8). The definition of η_i in (6) then implies the form (11) for the F_ρ-invariant manifold. In the sequel, this $(2n-k)$-dimensional submanifold is called the *manifold of partially synchronized states* of the coupled system. If $k = n$, the manifold $M := M(n)$ is simply called the *synchronization manifold.* □

In states, that are only synchronized in the generalized sense, the coordinates η_i of the synchronized units do not need to vanish. Conditions for generalized partial synchronization are given in the next lemma.

Lemma 2 *Suppose that the conditions of lemma 1 hold for some index set I_s with $k_s := |I_s|$. Let $I_g = \{i_1, \ldots, i_k\}$ be a further index set of $k := |I_g|$, $k \leq n - k_s$, and $I_g \cap I_s = \emptyset$. Assume that the parameter sets ρ^A, ρ^B and the coupling structure (w^{AB}, w^{BA}) of the modules A and B satisfy the following conditions for $m = 1, \ldots, k$:*

$$(w^A_{i_m j} - w^{BA}_{i_m j}) = (w^B_{i_m j} - w^{AB}_{i_m j}) \quad \textit{if} \quad j \in I_s\,, \tag{12}$$

$$w^A_{i_m j} = w^{BA}_{i_m j}\,,\ w^B_{i_m j} = w^{AB}_{i_m j} \quad \textit{if} \quad j \in \{1, \ldots, n\} \setminus I_s\,. \tag{13}$$

Then there exists a generalized partially synchronized dynamics constrained to a (2n-k)-dimensional F_ρ-invariant manifold

$$\widetilde{M}(k) := \{(a,b) \in \mathbf{R}^{2n} \mid a_{i_m} - b_{i_m} = c_{i_m}\,, c_{i_m} = \textit{constant},\ m = 1, \ldots, k\}\,.$$

If $k = n$, then there exist orbits of F_ρ constrained to an n-dimensional manifold; i.e., there exists a generalized synchronous dynamics.

Proof: First note, that the conditions (9) and (10) in lemma 1 constrain parameters for different i in (8) than conditions (12) and (13) in lemma 2 do; this is, because $I_s \cap I_g = \emptyset$. Thus, parameters are not restricted twice and therefore, they are well defined. Non-constrained parameters for units i in (8) with $i \in \{1, \ldots, n\} \setminus (I_s \cup I_g)$ are, of course, arbitrary. Note further that lemma 1 garantees the existence of a partially synchronous submanifold $M(k_s)$ for components in I_s. This submanifold can be empty, i.e. $k_s = 0$. All η_i, $i \in I_s$ are zero for orbits in $M(k_s)$. Inserting this, (12) and (13) into (8) for $i \in I_g$ it follows that $\sqrt{2} \cdot \eta_{i_m} = (\theta^A_{i_m} - \theta^B_{i_m}) = c_{i_m}$, $c_{i_m} = \textit{constant}$, $m = 1, \ldots, k$ for orbits starting in $M(k_s)$. Therefore, components a_{i_m} and b_{i_m}, $m = 1, \ldots, k$ are synchronized in the generalized sense and can be chosen to define the submanifold $\widetilde{M}(k)$ in lemma 2. Furthermore, the homeomorphism $\Phi : \mathbf{R}^k \to \mathbf{R}^k$ of definition 1 can obviously be realized by $b_{i_m} = a_{i_m} - (\theta^A_{i_m} - \theta^B_{i_m})$, $m = 1, \ldots, k$. □

Note 1: In the formulation of the dynamics of coupled neuromodules, and therefore also in lemmas 1 and 2, we have assumed that inputs θ into module neurons are stationary. Inspecting the proofs of lemmas 1 and 2, one easily sees,

that this restriction can be weakened. The lemmas both remain valid, if the inputs are time-dependend, $\theta(t)$, such that synchronization conditions hold for all times t - e.g. $\theta^A_{i_m}(t) = \theta^B_{i_m}(t),\ t = 0, 1, \ldots$ in (9).

Note 2: From lemma 1 and lemma 2 it follows that a generalized partial synchronization will occur if the coupling conditions are satisfied and some but not all θ_i are identical. The lemmas apply, of course, to different special situations: for instance, to a one-way coupling $(0, w^{BA})$, where a module A drives a module B, i.e. $w^{AB} = 0$, and the conditions for partial synchronization read

$$\theta^A_i = \theta^B_i\ , \quad (w^A_{ij} - w^{BA}_{ij}) = w^B_{ij}\ , \quad i,\, j = 1, \ldots, k \tag{14}$$

$$w^A_{ij} = w^{BA}_{ij}\ ,\ w^B_{ij} = w^{AB}_{ij}\ , \quad i = 1, \ldots, k\,,\ j = k+1, \ldots, n\ . \tag{15}$$

Another special case is that of identical systems coupled symmetrically; i.e.

$$\theta^A = \theta^B\ , \quad w^A = w^B\ , \quad w^{BA} = w^{AB}\ . \tag{16}$$

With $s_i := a_i = b_i$, $i = 1, \ldots, k$, and $l = k+1, \ldots, n$, the $(2n-k)$-dimensional partially synchronized dynamics on $M(k)$, denoted by $F_\rho|_M$, is given by the equations

$$\begin{aligned} s_i(t+1) = \theta_i \ &+ \ \sum_{j=1}^{k} w^+_{ij}\, \sigma(s_j(t)) \\ &+ \ \sum_{l=k+1}^{n} w^A_{il}\, \sigma(a_l(t)) + \sum_{l=k+1}^{n} w^B_{il} \cdot \sigma(b_l(t))\ , \end{aligned} \tag{17}$$

$$\begin{aligned} a_l(t+1) = \theta^A_l \ &+ \ \sum_{i=1}^{k} (w^A_{li} + w^{AB}_{li})\, \sigma(s_i(t)) \\ &+ \ \sum_{m=k+1}^{n} w^A_{lm}\, \sigma(a_m(t)) + \sum_{m=k+1}^{n} w^{AB}_{lm}\, \sigma(b_m(t))\ , \end{aligned} \tag{18}$$

$$\begin{aligned} b_l(t+1) = \theta^B_l \ &+ \ \sum_{i=1}^{k} (w^B_{li} + w^{BA}_{li})\, \sigma(s_i(t)) \\ &+ \ \sum_{m=k+1}^{n} w^{BA}_{lm}\, \sigma(a_m(t)) + \sum_{m=k+1}^{n} w^B_{lm}\, \sigma(b_m(t))\ , \end{aligned} \tag{19}$$

where $\theta_i := \theta^A_i = \theta^B_i$, and the *synchronization matrix* in (17) is defined as

$$w^+_{ij} := (w^A_{ij} + w^{AB}_{ij}) = (w^B_{ij} + w^{BA}_{ij}), \quad i, j = 1, \ldots, k. \tag{20}$$

This follows directly from (7) and the synchronization conditions (9) and (10). Correspondingly, the matrix appearing in the condition (9) is called the *obstruction matrix*

$$w^-_{ij} := (w^A_{ij} - w^{BA}_{ij}) = (w^B_{ij} - w^{AB}_{ij}), \quad i, j = 1, \ldots, k\,. \tag{21}$$

In general the partially synchronized dynamics $F_\rho|_M$ may have fixed point attractors as well as periodic, quasiperiodic or chaotic attractors, all constrained to M. Although the persistence of a partially synchronized dynamics is guaranteed by conditions (9) and (10), it is not at all clear that the dynamics (17) is asymptotically stable with respect to the dynamics F_ρ. Thus, a periodic or chaotic orbit in M may be an attractor for the partially synchronized dynamics $F_\rho|_M$ but not for the global dynamics F_ρ of the coupled system [4]. If the dynamics constrained to M is an attractor for F_ρ, then this partially synchronized dynamics is asymptotically stable in the sense, that small perturbations will not desynchronize the system.

To discuss stability aspects of the dynamics constrained to M, it is effective to use Lyapunov exponent techniques; i.e. we consider the *synchronization exponents* λ_i^s, $i = 1, \ldots, (2n-k)$, and the *transversal exponents* $\lambda_j^\perp$, $j = 1, \ldots, k$. The synchronization exponents λ_i^s are just the $(2n-k)$ Lyapunov exponents of the dynamics $F_\rho|_M$ on M given by equations (17) to (19). The transversal exponents $\lambda_j^\perp$, $j = 1, \ldots, k$ are calculated as Lyapunov exponents with respect to the partial linearization

$$L_{ij}^-(s) := w_{ij}^- \cdot \sigma'(s_j)\,, \quad i,j = 1, \ldots, k\,, \tag{22}$$

of F_ρ along partially synchronized states $(\xi, \eta))$, where w^- denotes the obstruction matrix (21).

Partially synchronized chaotic dynamics will be characterized by a situation where the largest synchronization exponent λ_1^s is positive; i.e. $\lambda_1^s > 0$. On the other hand, an unstable partially synchronized dynamics on M will be characterized by a largest transversal exponent $\lambda_1^\perp(s)$ satisfying $\lambda_1^\perp > 0$. Thus, if a stable manifold M, containing a chaotic orbit, will turn unstable, then the coupled system will enter a hyperchaotic regime [42]; i.e. at least two Lyapunov exponents of the coupled system are positive.

For the special case of completely synchronized dynamics, i.e. $k = n$, exponents λ_i^s and $\lambda_j^\perp$ are derived from the linearizations

$$L_{ij}^\pm(s) := w_{ij}^\pm \cdot \sigma'(s_j)\,, \quad i,j = 1, \ldots, n\,, \tag{23}$$

respectively, with w^+ the synchronization matrix (20), and w^- the obstruction matrix (21).

If the matrix w^- has only zero eigenvalues, then also the linearization $L^-(s(t))$ will have zero eigenvalues along a partially synchronized orbit $s(t)$, and it follows that the transversal exponents $\lambda_j^\perp$, $j = 1, \ldots, k$, are all negative. Thus, the partially synchronized dynamics will be stable for all parameter values satisfying conditions (9) and (10), and the corresponding coupling structure (w^{AB}, w^{BA}) of modules will be called *stabilizing*. Especially, if w^- is the zero matrix, we call (w^{AB}, w^{BA}) *minimal*. A minimal coupling structure is always stabilizing a partially synchronous dynamics.

To destabilize a partially synchronized dynamics of degree k, eigenvalues of w^- must be nonzero and large enough to make contributions to the positivity of the largest transversal exponent $\lambda_1^\perp$. The de-stabilizing property depends furthermore on the density of an orbit around the partially synchronized states satisfying $s_i = 0$, $i = 1, \ldots, k$.

3 Example 1: Coupling different 3-modules

Numerical examples for the existence of complete synchronization of coupled neuromodules where given, for example, in [36] for symmetrically coupled identical systems. Our first example will demonstrate that generalized and partial as well as complete synchronization can also be observed for coupling of different subsystems.

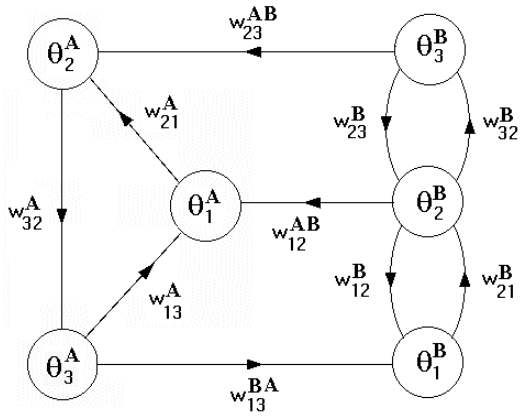

Figure 1: A minimal coupling configuration for complete synchronization of a 3-ring (module A) with a bidirectional 3-chain (module B).

To this end we choose the following setup where a 3-ring is coupled to a bi-directional 3-chain. The dynamical features of the isolated systems are quite different: besides fixed point attractors 3-rings can have period-2, -3 and period-6 attractors [34], whereas 3-chains can have p-periodic attractors for all p as well as chaotic attractors [33]. Nonetheless there are many different coupling schemes which guarantee the existence of synchronized dynamics. We choose modules and couplings as shown in figure 1. The corresponding dynamics of the coupled system is then given by

$$\begin{aligned} a_1(t+1) &:= \theta_1^A + w_{13}^A\,\sigma(a_3(t)) + w_{12}^{AB}\,\sigma(b_2(t))\,, \\ a_2(t+1) &:= \theta_2^A + w_{21}^A\,\sigma(a_1(t)) + w_{23}^{AB}\,\sigma(b_3(t))\,, \\ a_3(t+1) &:= \theta_3^A + w_{32}^A\,\sigma(a_2(t))\,, \end{aligned} \tag{24}$$

$$
\begin{aligned}
b_1(t+1) &:= \theta_1^B + w_{12}^B\,\sigma(b_2(t)) + w_{13}^{BA}\,\sigma(a_3(t))\ , \\
b_2(t+1) &:= \theta_2^B + w_{21}^B\,\sigma(b_1(t)) + w_{23}^B\,\sigma(b_3(t))\ , \\
b_3(t+1) &:= \theta_3^B + w_{32}^B\,\sigma(b_2(t))\ .
\end{aligned}
$$

If, according to (9) and (10), the following conditions are satisfied,

$$
w_{12}^B = w_{12}^{AB}\ , \quad w_{13}^A = w_{13}^{BA}\ , \quad w_{21}^A = w_{21}^B\ , \quad w_{23}^B = w_{23}^{AB}\ , \quad w_{32}^A = w_{32}^B\ ,
$$

$$
\theta_1^A = \theta_1^B\ , \quad \theta_2^A = \theta_2^B\ , \quad \theta_3^A = \theta_3^B\ ,
$$

then a completely synchronized dynamics exists for this configuration. This has been reported in [37]. It is easy to check that the corresponding obstruction matrix w^- has zero eigenvalues for all parameter values. Thus, the completely synchronized dynamics is always stable. For the same coupled 3-modules we will now study the generalized partial synchronized dynamics of different types and degrees.

3.1 Partial synchronization of degree 1

To start with, we look for a partial synchronization of degree 1 for neurons 1^A and 1^B. According to lemma 2, i.e. conditions (9) and (10), parameters have to satisfy

$$
\theta_1^A = \theta_1^B\ , \quad w_{12}^B = w_{12}^{AB}\ , \quad w_{13}^A = w_{13}^{BA}\ . \tag{25}
$$

This can be realized, for instance, by setting the coupling connection w_{23}^{AB} in the original configuration shown in figure 1 to zero. Other parameter values are arbitrary; we choose inputs of the modules and nonzero weights as follows

$$
\begin{aligned}
\theta_1 &= -0.7\ , \quad \theta_2 = -0.5\ , \quad \theta_3 = -4\ , \quad \text{and} \quad w_{12}^B = w_{12}^{AB} = 8\ , \\
w_{21}^A &= w_{21}^B = w_{32}^A = w_{32}^B = 8\ , \quad w_{13}^A = w_{13}^{BA} = w_{23}^B = w_{23}^{AB} = -8\ .
\end{aligned} \tag{26}
$$

For these parameters figure 2 displays the dynamics of the system in form of projections of the 6-dimensional phase-space to different subspaces: in the upper left corner the (o_1^A, o_2^A)-subspace of module A is shown, whereas the other three frames display activities of corresponding neurons in the modules A and B, (o_1^A, o_1^B), (o_2^A, o_2^B), (o_3^A, o_3^A).

First of all, the irregular attractor structure in the (o_1^A, o_2^A)-plot shows, that the dynamics inside module A is chaotic, a fact that we also confirmed by calculating Lyapunov exponents. Similarly, the dynamics projected to module B is chaotic (not shown); but since the modules have different connectivity, projections of chaotic attractors to modules A and B are in general not identical.

Nonetheless, as seen in the lower left frame of figure 2, neurons 1 in both modules are synchronized, that is, o_1^A maps identically to o_1^B. In contrast the second

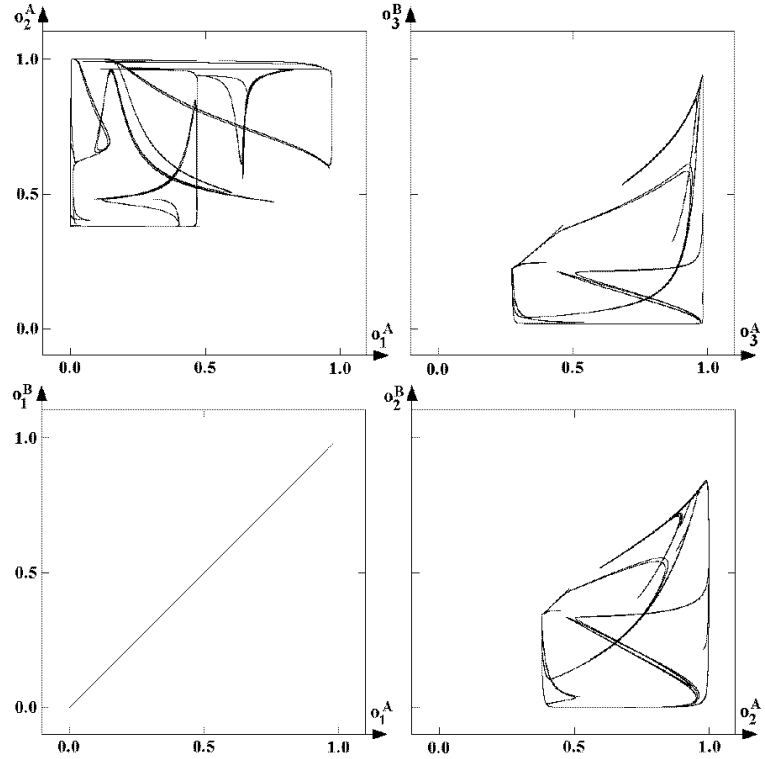

Figure 2: Partially synchronized chaos of degree 1 for two coupled 3-modules having different architectures. Parameters: see text.

and third components of the coupled modules are not synchronized; their dynamics in the common subspaces reveal a more complex relationship. Hence, in the present example, the 6-dimensional dynamics of the coupled system is constrained to a 5-dimensional partially synchronized chaotic attractor. As a further fact (not seen in the figure) this chaotic attractor coexists with a partially synchronized period-4 attractor. The 5-dimensional partially synchronized dynamics (17) of this configuration will be stable for all parameter values, because the corresponding obstruction matrix (21) satisfies $w_{11}^- = 0$. That the 5-dimensional dynamics is highly non-trivial can be read from its bifurcation diagram shown in figure 3 for the above given parameter values (26), but with varying $\theta_1 := \theta_1^A = \theta_1^B$: Starting from a fixed point attractor at $\theta_1 = -3$ a bifurcation to quasiperiodic attractors occurs around $\theta_1 = -2.4$, and, after that, various windows for periodic and chaotic attractors are visible. Furthermore, over a large parameter domain the shown attractors coexist with a sequence of p-periodic attractors with periods $p \leq 4$. All coexisting attractors are partially synchronized; thus, partial synchronization exists over large parameter regions.

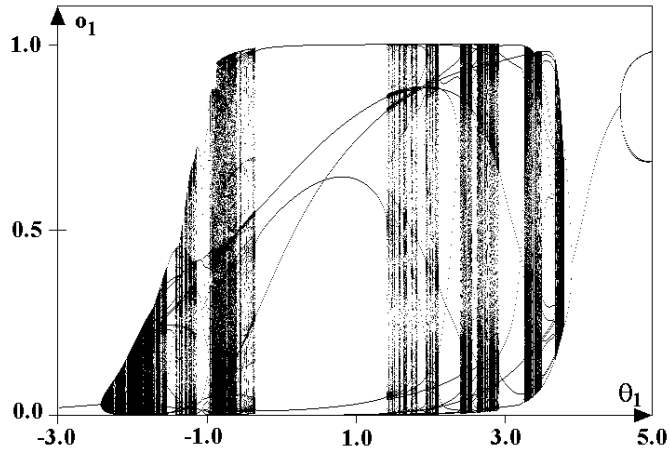

Figure 3: A bifurcation diagram for the partially synchronized dynamics of degree 1 with respect to θ_1. Fixed parameters for coupled 3-modules: see text.

3.2 Generalized partial synchronization of degree 1

We now look for a generalized partial synchronization of degree 1 for neurons 1^A and 1^B, where these neurons are not perfectly synchronous, but are still constrained to a one-dimensional manifold. According to lemma 1 the condition simply reads

$$w_{13}^A = w_{13}^{BA} \ ,$$

the other parameters are arbitrary. Furthermore, the proof of lemma 1 shows that the homeomorphism $\Phi : \mathbf{R}^1 \to \mathbf{R}^1$, mapping the first component of module A to the corresponding first component of module B is given by the linear relation

$$b_1 = (\theta_1^B - \theta_1^A) + a_1 \ . \tag{27}$$

Figure 4, as in the previous example, displays projections of a partially synchronized chaotic attractor of degree 1 to the phase spaces of corresponding neuron pairs, as well as to the subspace (o_1^A, o_2^A) of module A. The parameter values for this chaotic attractor are:

$$w_{12}^B = w_{12}^{AB} = w_{21}^A = w_{21}^B = w_{32}^A = w_{32}^B = 8 \ ,$$

$$w_{13}^A = w_{13}^{BA} = w_{23}^B = w_{23}^{AB} = -8 \ ,$$

$$\theta_1^A = -0.8,\ \theta_1^B = -2 \ , \quad \theta_2^A = 5.3,\ \theta_2^B = 6.1, \quad \theta_3^A = -5,\ \theta_3^B = -4 \ .$$

Observe that, in contrast to the previous example, the neurons 1_A and 1_B are now only synchronized in the generalized sense - the mapping between their outputs is not the identity but some other non-linear bijective functional relationship. (Note, that this relationship does not have the simple linear form (27). This is, because figure 4 displays output values, $o_1^A = \sigma(a_1)$ and $o_1^B = \sigma(b_1) =$

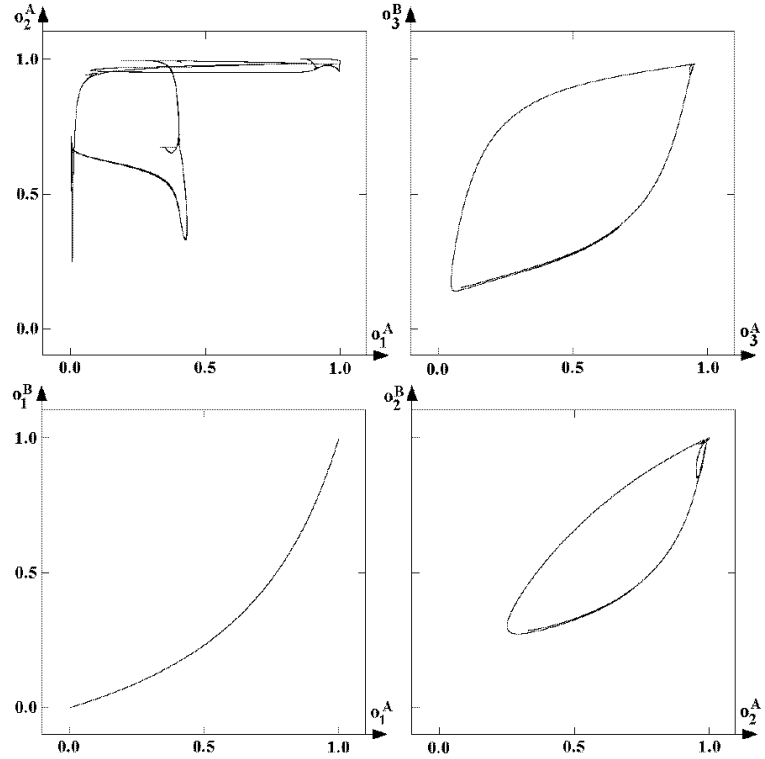

Figure 4: Projections of a generalized partially synchronized chaotic attractor of degree 1 for coupled 3-modules. Parameters: see text.

$\sigma(\theta_1^B - \theta_1^A + a_1)$.) Again, bifurcation diagrams (not shown) reveal that also a complex (periodic, quasiperiodic, and chaotic attractors) generalized synchronous dynamics of degree 1 exists for large parameter domains in this setup.

3.3 Generalized and partial synchronization

Lemma 2 tells us that a generalized synchronization of modules may be realized with some of the components being exactly synchronized. To demonstrate this case, where a generalized synchronous dynamics is at the same time partially synchronous, we choose the following example. Synchronization conditions (9) and (10) for partial synchronization of degree 2 of the coupled 3-ring and 3-chain read

$$w_{12}^B = w_{12}^{AB} \ , \quad w_{13}^A = w_{13}^{BA} \ , \quad w_{21}^A = w_{21}^B \ , \quad w_{23}^B = w_{23}^{AB} \ , \qquad (28)$$
$$\theta_1^A = \theta_1^B \ , \quad \theta_2^A = \theta_2^B \ .$$

Figure 5 shows a realization of partial synchronization of degree 2 for the nonzero parameter values

$$\begin{aligned} w_{12}^B &= w_{12}^{AB} = w_{21}^A = w_{21}^B = w_{32}^A = 8 \ , \quad w_{13}^A = w_{13}^{BA} = w_{23}^B = w_{23}^{AB} = -8 \ , \\ w_{32}^B &= 11 \ , \quad \text{and} \quad \theta_1 = -0.5 \ , \quad \theta_2 = -3.3 \ , \quad \theta_3^A = -6 \ , \quad \theta_3^B = -4 \ . \end{aligned} \qquad (29)$$

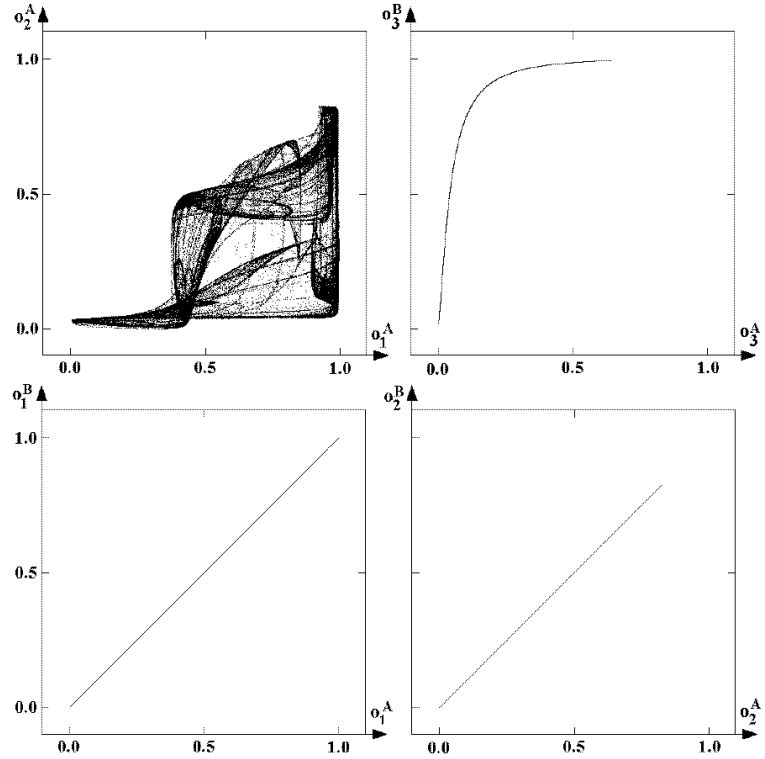

Figure 5: Partially synchronized chaos of degree 2 for two coupled 3-modules having different architectures. Parameters: see text.

Again projections of the corresponding chaotic dynamics to subspaces (o_1^A, o_2^A), (o_1^A, o_1^B), (o_2^A, o_2^B), and (o_3^A, o_3^B) are shown, demonstrating the synchronous activity of neuron pairs $(1^A, 1^B)$ and $(2^A, 2^B)$. As this figure suggests, in addition to partial synchronization, according to definition (1), this is at the same time an example for a generalized dynamics of two modules. In fact, the resulting dynamics of the coupled system is not 4-dimensional - as expected - but it is still constrained to a 3-dimensional manifold as can be seen from the (o_3^A, o_3^B) plot. Although the conditions (28) do not match the conditions (12) and (13) of theorem 2 - we have $8 = w_{32}^A \neq w_{32}^B = 11$ - this is because we can write the dynamics of module B still as a map of the dynamics of module A as follows:

$$b_1 = a_1 \ , \quad b_2 = a_2 \ , \quad b_3 = \theta_3^B + \frac{w_{32}^B}{w_{32}^A} \left(a_3 - \theta_3^A \right) \ .$$

The obstruction matrix w^- (21) for this configuration has again zero eigenvalues, so that the partially synchronized dynamics will be always stable. Bifurcation diagrams for this 3-dimensional dynamics (not shown) again reveal that this dynamics is highly nontrivial and has periodic as well as quasiperiodic and chaotic attractors, all constrained to a 3-dimensional manifold.

4 Example 2: Partial synchronization of modules having different numbers of neurons

Partial synchronization can appear also if the two coupled modules have different numbers of neurons. To fit the general formalism of section 2, we just have to add as many isolated neurons to one module such that both modules formally have the same number of neurons. To demonstrate this, we choose the following setup where a chaotic 2-module (module A) is coupled to a bi-directional 3-chain (module B). The dynamics of the isolated modules is given by the equations

$$\begin{aligned} a_1(t+1) &:= \theta_1^A + w_{12}^A\,\sigma(a_2(t))\;, \\ a_2(t+1) &:= \theta_2^A + w_{21}^A\,\sigma(a_1(t)) + w_{22}^A\,\sigma(a_2(t))\;, \end{aligned} \tag{30}$$

$$\begin{aligned} b_1(t+1) &:= \theta_1^B + w_{12}^B\,\sigma(b_2(t))\;, \\ b_2(t+1) &:= \theta_2^B + w_{21}^B\,\sigma(b_1(t)) + w_{23}^B\,\sigma(b_3(t))\;, \\ b_3(t+1) &:= \theta_3^B + w_{32}^B\,\sigma(b_2(t))\;. \end{aligned} \tag{31}$$

We now look for the partially synchronized dynamics of these two coupled modules.

4.1 Partial synchronization of degree 1

In the first case we want to synchronize the dynamics of neuron 1^A with neuron 1^B. The synchronization conditions (9) and (10) lead, for example, to a configuration shown in figure 6, with parameters satisfying

$$\theta_1^A = \theta_1^B, \quad w_{12}^A = w_{12}^{BA}, \quad w_{12}^B = w_{12}^{AB}\;. \tag{32}$$

We observed interesting bifurcation scenarios for the corresponding partially synchronized dynamics; for instance, from a fixed point attractor to a period-2 attractor which then bifurcates into a 2-cyclic quasiperiodic attractor. With growing input θ_1 windows for periodic as well as chaotic attractors are observed. As an example, in figure 7 a chaotic attractor with synchronized neurons 1^A and 1^B is shown. Parameters for this attractor have values

$$\begin{aligned} w_{12}^A = w_{12}^{BA} = w_{12}^B = w_{12}^{AB} = w_{23}^B = -6\,, w_{21}^A = w_{21}^B = w_{32}^B = 6\,, \\ w_{22} = -16\,, \quad \theta_1 = \theta_1^A = \theta_1^B = 3\;, \quad \theta_2^A = \theta_2^B = -2\;, \quad \theta_3^B = 0.5\,. \end{aligned} \tag{33}$$

Clearly seen is that neurons 1^A and 1^B are synchronized and 2^A and 2^B are not synchronized. The projection of the chaotic dynamics to the phase space (o_1^A, o_2^A) of module A is seen in the upper left part. Because the obstruction matrix satisfies $w^- = w_{11}^- = 0$, the partial synchronization in this configuration

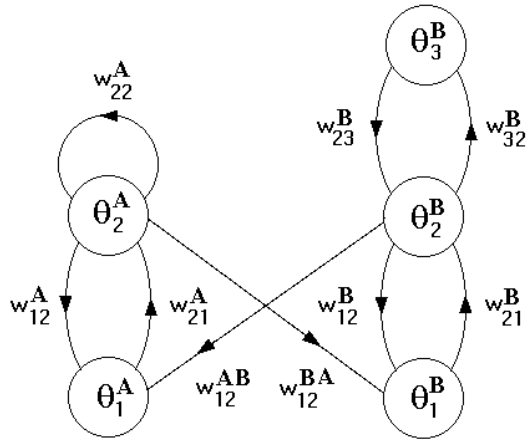

Figure 6: Coupling scheme for partial synchronization of degree 1 of a 2-neuron with a 3-neuron network. Parameters: see text.

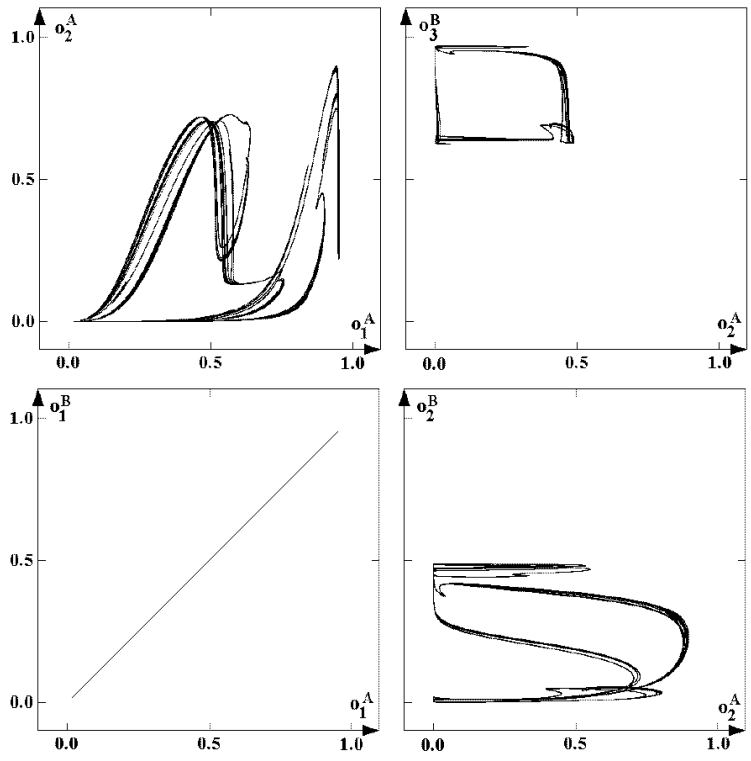

Figure 7: A global chaotic attractor of the coupled system shown in figure 6 with synchronized units 1^A and 1^B. Parameters: see text.

is stable for all allowed parameter values. As follows from the synchronization conditions, synchronization of neurons 1^A and 1^B persists even if weights $w_{12}^A = w_{12}^{BA}$, $w_{21}^{AB} = w_{21}^B$, w_{23}^B, and w_{32}^B are varying independently. Most interestingly, the same holds true for independent variations of the (constant) inputs θ_2^A, θ_2^B, and θ_3^B. Moreover, according to Note 1 above, as long as $\theta_1^A(t) = \theta_1^B(t)$ holds for every time step t, the partial synchronization will persist in time independent of the other inputs. Those inputs of course influence the orbit of the coupled system in phase space, but they do not desynchronize the dynamics.

4.2 Partial synchronization of degree 2

Synchronization conditions (9) and (10) for the degree 2 case are satisfied e.g. by an architecture shown in figure 8 with parameters satisfying

$$\theta_1^A = \theta_1^B, \quad \theta_2^A = \theta_2^B, \quad w_{12}^A = w_{12}^B, \quad w_{21}^A = w_{21}^B, \quad w_{22}^A = w_{22}^{BA}, \quad w_{23}^B = w_{23}^{AB} .$$

This configuration exhibits a partially synchronized chaotic attractor of degree

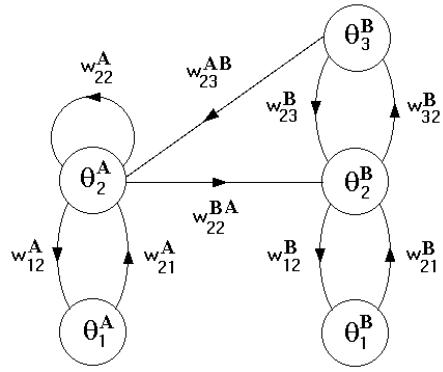

Figure 8: Coupling configuration for a partial synchronization of degree 2 of a 2-neuron with a 3-neuron network. Parameters: see text.

2 for the following values:

$$w_{12}^A = w_{12}^B = w_{23}^{AB} = w_{23}^B = -6 , \quad w_{21}^A = w_{21}^B = w_{32}^B = 6 , \quad w_{22}^A = w_{22}^{BA} = -16 ,$$

$$\theta_1 = \theta_1^A = \theta_1^B = 3 , \quad \theta_2^A = \theta_2^B = -2 , \quad \theta_3^B = 0.5 .$$

The synchronous activity of neuron pairs $(1^A, 1^B)$ and $(2^A, 2^B)$ can be clearly seen in projections of this attractor to corresponding subspaces shown in figure 9. The partially synchronized dynamics for this coupling structure is stable for all allowed parameter values, because its obstruction matrix w^- has zero eigenvalues. Again we observe stable partially synchronized dynamics with non-trivial bifurcation sequences including fixed point attractors as well as periodic, quasiperiodic and chaotic attractors.

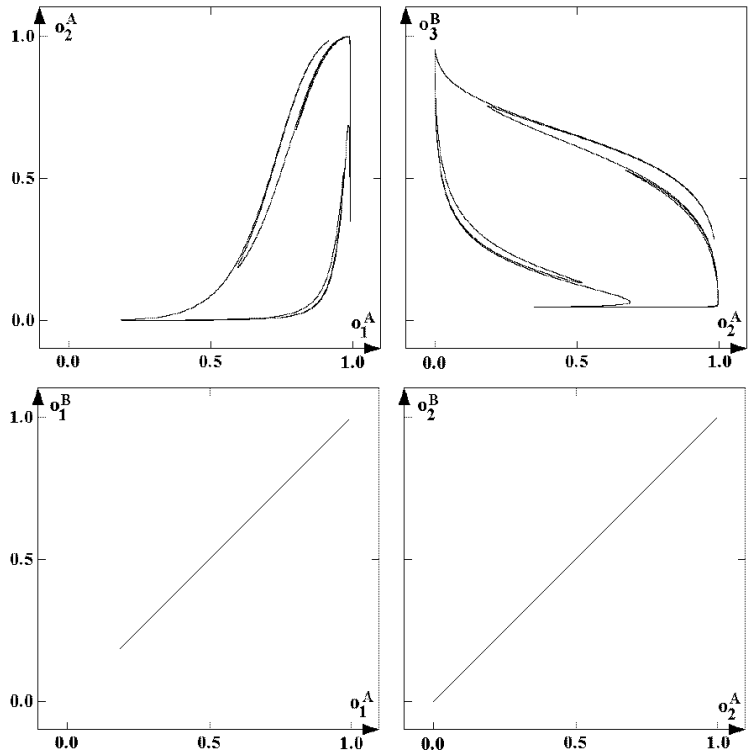

Figure 9: A partially synchronized chaotic attractor of degree 2 for the coupled system shown in figure 8. Parameters: see text.

4.3 Unstable synchronized dynamics

In the examples given above the coupling structure (w^{AB}, w^{BA}) was always stabilizing the synchronous dynamics. Using the system of the last section 4.2, we want to show that introducing just one more coupling connection between modules will allow - besides stable synchronization of neurons - also an unstable synchronized dynamics. This additional connection has to be chosen in such a way that the corresponding obstruction matrix w^- can have nonzero eigenvalues. In the coupled system shown in figure 8 this can be achieved by introducing the weight w_{22}^{BA} satisfying the synchronization condition; i.e. $(w_{22}^A - w_{22}^{BA}) = w_{22}^{AB} \neq 0$. Then the (2×2) obstruction matrix has nonzero components $w_{12}^- = w_{12}^A$, $w_{21}^- = w_{21}^A$, and $w_{22}^- = (w_{22}^A - w_{22}^{BA})$.

We calculate the transversal Lyapunov exponent $\lambda^\perp$ for the corresponding 3-dimensional synchronized dynamics

$$\begin{aligned} s_1(t+1) &= \theta_1 + w_{12}^+ \, \sigma(s_2) \, , \\ s_2(t+1) &= \theta_2 + w_{21}^+ \, \sigma(s_1) + w_{22}^+ \, \sigma(s_2) + w_{23}^+ \, \sigma(b_3) \, , \\ b_3(t+1) &= \theta_3^B + w_{32}^B \, \sigma(s_2) \, . \end{aligned} \tag{34}$$

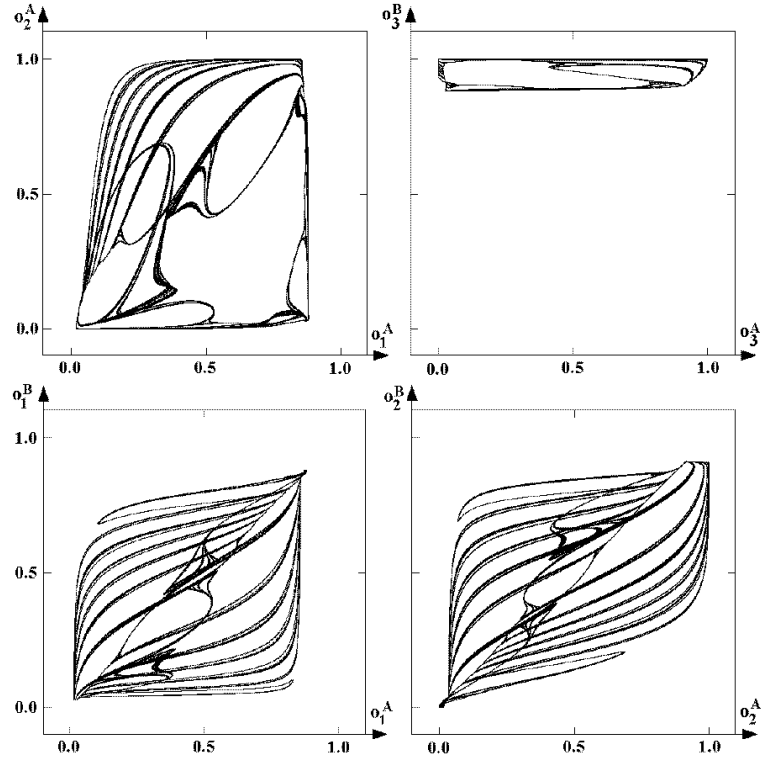

Figure 10: An asynchronous chaotic attractor for parameters (see text) where the partially synchronized dynamics is unstable.

with $\theta_1 = \theta_1^A = \theta_1^B$, $\theta_2 = \theta_2^A = \theta_2^B$, and use the convenient parameter values

$$\begin{aligned} w_{12}^+ &= -6\,, \quad w_{21}^+ = w_{32}^B = 6\,, \quad w_{22}^A = -16\,, \quad w_{22}^{AB} = 11\,, \\ w_{22}^{BA} &= -5\,, \quad w_{22}^+ = -11\,, \quad \theta_1 = 2\,, \quad \theta_2 = 2.5\,, \quad \theta_3^B = 2\,. \end{aligned} \tag{35}$$

Then, the obstruction matrix has nonzero components $w_{12}^- = -6$, $w_{21}^- = 6$, and $w_{22}^- = -11$.

In figure 10 an asynchronous chaotic attractor is depicted for parameter values as given above in (35), which is visible instead of the unstable partially synchronized quasiperiodic dynamics predicted by (34). Unstability of the partially synchronized dynamics can be read also from figure 13, where the largest transversal Lyapunov exponent is shown to be positive for $\theta_1 = 2$.

Figure 11 shows the bifurcation diagram with respect to varying inputs θ_1 for the corresponding partially synchronized dynamics of degree 2 defined by (34). It shows a bifurcation from a fixed point attractor to quasiperiodic dynamics followed by a window of period-3 attractors. Before the dynamics ends up in period-2 attractors there is a window of a period-3 attractors coexisting with quasiperiodic and fixed point attractors. Not all of these attractors are stable, that is, attractors of the full 6-dimensional dynamics.

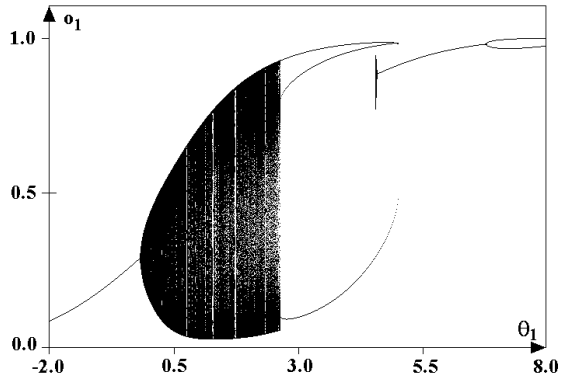

Figure 11: A bifurcation diagram for the (stable and unstable) partially synchronized dynamics of degree 2 with respect to θ_1.

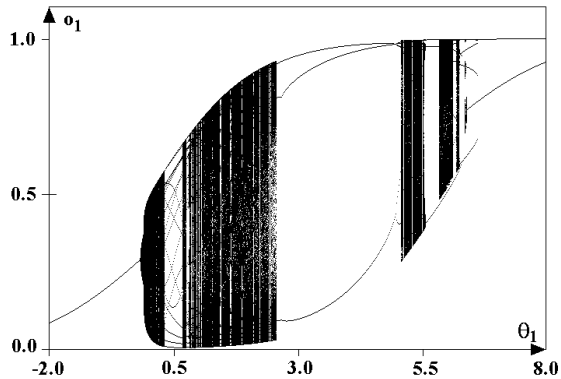

Figure 12: A bifurcation diagram for the observed (synchronous and asynchronous) dynamics with respect to slowly varying θ_1.

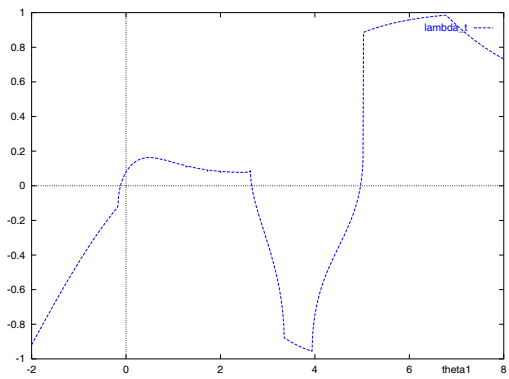

Figure 13: Transversal Lyapunov exponents for the partially synchronized dynamics of degree 2 with respect to θ_1.

This is demonstrated in figure 12 by the corresponding bifurcation diagram for the "observable" asymptotic dynamics of the coupled system. It reveals a quite different behavior: At first it follows the synchronous behavior in bifurcating from a fixed point attractor to a quasiperiodic one, but shortly afterwards it bifurcates to an asynchronous quasiperiodic attractor, followed by a window of periodic attractors with higher periods, and then a chaotic domain. Around $\theta_1 = 2.5$ it enters again the stable synchronized period-3 domain, and bifurcates to asynchronous chaotic attractors and periodic attractors around $\theta_1 = 5$. This sequence of stable and unstable partially synchronized dynamics can be followed at the same time by the behavior of the largest transversal Lyapunov exponent $\lambda_1^{\perp}$ which is displayed in figure 13.

5 Discussion

In summary, we have shown that synchronized activity of groups of neurons in a system of coupled recurrent neural networks is always achievable, if the sum of bias terms and stationary external inputs to corresponding module neurons are identical, and coupling connections are set appropriately. Furthermore, the coupled networks can be of different type and dimension. The partially synchronized dynamics of the coupled system is describable as that of an isolated neuromodule C^+ with weight matrix given by the so-called synchronization matrix w^+. The reduced system is typically - although not necessarily - different from each of the coupled systems. Depending on the module parameters of C^+ (weights and bias terms/stationary inputs), the partially synchronized orbits can be periodic, quasiperiodic or chaotic. The synchronization will be stable, if these orbits, constrained to the manifold of partially synchronized states, are attractors for the dynamics of the coupled system. Otherwise it is unstable. Stability of a partially synchronized dynamics can be checked numerically by calculating the largest transversal Lyapunov exponent which is determined by the so-called obstruction matrix w^-.

Taking the experiences with completely synchronized neuromodules into account [36], one has to realize that for large parameter domains stable synchronous dynamics will co-exist with asynchronous periodic, quasiperiodic or even chaotic attractors. Thus, whether a system ends up asymptotically in a partially synchronous mode or not depends crucially on initial conditions, i.e. on the internal state of the system. In this sense the reaction to external signals depends also on the *history* of the system itself. This introduces *memory effects* into the behavior of coupled systems. Furthermore, a synchronized mode often persists even if external inputs are time dependent.

Desynchronization of module dynamics can be achieved in different ways. From the synchronization conditions (9) and (10) it is clear that diverging external inputs or other inappropriate parameter settings (module weights or coupling

strengths) will immediately desynchronize the modules. Depending on the coupling conditions a mode of lower degree of synchronization may be reached or the system may completely desynchronize.

Different from this standard situation, certain external signals may also be used to drive the composed system into domains where the - still existing - synchronized dynamics gets unstable. In such unstable parameter domains, synchronization is particularly sensitive to perturbations transversal to the synchronization manifold; hence, appropriate control signals may be used to transiently modulate the responsiveness of the coupled network to reach quick and active desynchronization of modules reacting to slightly different input signals. On the other hand, varying the inputs of non-synchronized neurons will not effect the presence of partial synchronization; it will just alter occasionally the type of the synchronized dynamics, following, for instance, a bifurcation sequence.

Putting things together, synchronization of a specific group of neurons in response to external specific stimuli depends in a complex way on the connectivity of the system, on the internal state (the history) of the system, as well as the setting of other parameters, like inputs to non-synchronous neurons. Furthermore, parameter changes can select different types (periodic, chaotic) of partially synchronous dynamics in response to one and the same stimulus.

We have further shown that beside stable and unstable complete synchronization different types of generalized as well as partial synchronization can be realized in coupled neuromodules. According to lemma 1 and the displayed numerical examples, a generalized synchronous dynamics of coupled modules will appear if the synchronization conditions (9) and (10) for the connectivity are satisfied, and some but not all input/bias terms of corresponding neurons are identical. This is an interesting feature, because the *effective* dynamics of a coupled systems is constrained to a lower dimensional manifold, as it is the case for the synchronized dynamics, but the homeomorphism mapping one (sub)system to the other is no longer the identity. In addition, generalized synchronization can be further restricted to only parts of the coupled system (generalized partial synchronization). This way the spatio-temporal structure of the (generalized) synchronized signals can be changed continuously within stable parameter ranges or discontinuously at stability borders; effects which may in turn be used for neural coding (e.g. [29, 46, 44]). Because different constraining manifolds can be selected by different coupling schemes of modules, this may be also a versatile feature for shaping dynamic properties of neural and cognitive systems.

Parameters may also be used to decide, whether a system is responding to a given stimulus with a partially synchronous mode at all. Physiologically such parameters may be identified as subcortical input, which, for instance, is known to strongly modulate spatial ranges of synchronization of cortical oscillations in the alpha- and gamma-range (e.g. [41]). Alternatively, parameter changes may be represented by feedback from higher cortical areas either in the form of integrative input signals, that organize or 'bind' otherwise isolated local submodules into

larger functional networks [6, 14, 44], or as part of some attentional mechanism.

One should also note, that such feedback does not just provide electrical input into cortical cells. By varying excitability of cells, it is also capable to change the functional connectivity within the network [3]. This way different effective coupling schemes could be selected that support different kinds of collective dynamics. A similar role may also be played by neuromodulatory (e.g. the monoaminergic) transmitter systems in the brain. Their influence on functional connectivity as well as their capability to switch dynamical properties of complex collective modes of activation have repeatedly been demonstrated (e.g. [24, 26]).

The modules in this paper were composed of standard graded neurons. Results, however, are not restricted to networks of simple sigmoid neurons. Complex dynamics can similarly be observed in networks of "spiking neurons" ranging from simple integrate-and-fire cells to conductance based compartmental neuron models. Observed effects, so far, include complete, generalized, and partial synchronization, hysteresis, chaotic dynamics, and more [9, 11, 16, 23, 39, 45, 46, 48].

Although the theoretical analysis of networks of spiking neurons is considerably more difficult than the calculations presented in this paper and mathematical studies have been performed to date only for some restricted dynamical modes (mainly asynchronous firing and complete synchronization, see for example [18, 31, 47]), we expect that the collective dynamical modes of such networks are at least as abundant than those revealed by our simpler model systems.

We believe that the dynamical phenomenology of the presented results, although derived for formal neural networks, can stimulate the development of conceptually new dynamical models for cortical information processing or even cognitive capabilities [33]. As a direct application, the rather typical co-existence of synchronized modes with modes of asynchronous dynamics generalizes functional properties like "feature binding" often attributed to the synchronization of oscillations. At the same time it introduces memory aspects into these systems through generalized hysteresis effects. Furthermore, since synchronization and desynchronization of modules can be controlled by different parameters, attention-guided synchronization of subsystems is an additional interesting functional feature of coupled neuromodules.

References

[1] Abarbanel, H. D. I., Rulkov, N. F., and Sushchik, M. M. (1996) Generalized synchronization of chaos: The auxiliary system approach, *Phys. Rev. E*, **53**, 4528–4535.

[2] Abraham, R. H., Gardini, L. and Mira, C. (1997) *Chaos in Discrete Dynamical Systems*, Springer-Verlag, New York.

[3] Aertsen, A.M.H.J.; Gerstein, G.L.; Habib, M.K.; Palm, G. (1989) Dynamics of neuronal firing correlation - modulation of effective connectivity, *J. Neurophysiol.*, **61**, 900–917.

[4] Ashwin, P., Buescu, J., and Stewart, I. (1996) From attractor to chaotic saddle: a tale of transverse instability, *Nonlinearity*, **9**, 703–737.

[5] Blum, E. K., and Wang, X. (1992) Stability of fixed points and periodic orbits and bifurcations in analog neural networks, *Neural Networks*, **5**, 577–587.

[6] Bullier, J.; Munk, H.J.; Nowak, L.G. (1993) Cortico-cortical connections sustain interarea synchronization, *Concepts Neurosci.*, **4**, 159–174.

[7] Buzsáki, G.; Chrobak, J.J. (1995) Temporal structure in spatially organized neuronal ensembles: a role for interneuronal networks, *Current Opinion in Neurobiology*, **5**, 504–510.

[8] Chapeau-Blondeau, F., and Chauvet, G. (1992) Stable, oscillatory, and chaotic regimes in the dynamics of small neural networks with delay, *Neural Networks*, **5**, 735-743.

[9] Carroll, T. L. (1995), Synchronization and complex dynamics in pulse-coupled circuit models of neurons, *Biol. Cybern.*, **73**, 553 –559.

[10] Cuomo, K. M., and Oppenheim, A. V. (1993) Circuit implementation of synchronized chaos with applications to communications, *Phys. Rev. Lett.*, **71**, 65–68.

[11] Deppisch, J.; Bauer, H. U.; Schillen, T.; König, P; Pawelzik, K.; and Geisel, T. (1993) Alternating oscillatory and stochastic states in a network of spiking neurons, *Network*, **4**, 243–257.

[12] De Sousa Viera, M., and Lichtenberg, A. J. (1997) Nonuniversality of weak synchronization in chaotic systems, *Phys. Rev. E*, **56**, R3741–3744.

[13] Doyon, B. (1992) On the existence and the role of chaotic processes in the nervous system, *Acta Biotheor.*, **40**, 113–119.

[14] Eckhorn, R., Bauer, R., Jordan, W., Brosch, M., Kruse, W., Munk, M. and Reitboeck H.J. (1988) Coherent oscillations: a mechanism for feature linking in the visual cortex. *Biol. Cybern.*, **60**, 121–130.

[15] Engel, A. K., Roelfsma, P.R., Fries, P., Brecht, M. and Singer, W. (1997) Binding and response selection in the temporal domain - a new paradigm for neurobiological research? *Theory in Biosciences*, **116**, 241–266.

[16] Ernst, U.; Pawelzik, K.; Geisel, T. (1998) Delay-induced multistable synchronization of biological oscillators, *Phys.Rev. E*, **57**, 2150–2162.

[17] Gerstner, W., Ritz, R., and van Hemmen, J.L. (1993) A biologically motivated and analytically soluble model of collective oscillations in the cortex, I. Theory of weak locking, *Biol. Cybern* **68**, 363–374.

[18] Gerstner, W. (1995) Time Structure of the Activity in Neural Network Models, *Phys. Rev. E*, **51**, 738–758.

[19] Ghose, G.M. and Freeman, R.D. (1992) Oscillatory discharge in the visual system: does it have a functional role? *J. Neurophysiol.*, **68**, 1558–1574.

[20] Gray, C.M. (1994) Synchronous Oscillations in Neuronal Systems: Mechanisms and Functions, *J. Comp. Neurosci.*, **1**, 11–38.

[21] Guckenheimer, J., Gueron, S., and Harris-Warrick, R.M. (1993) Mapping the dynamics of a bursting neuron, *Philos. Trans. R. Soc. Lond. B (Biol Sci)*, **341**, 345–359.

[22] Hansel, D., and Sompolinsky H. (1992) Synchronization and computation in a chaotic neural network, *Phys. Rev. Lett.*, **68**, 718–721.

[23] Hansel, D., and Sompolinsky, H. (1996) Chaos and synchrony in a model of a hypercolumn in visual cortex, *J. of Computational Neuroscience*, **3**, 7–34.

[24] Harris-Warrick, R.M.; Marder, E. (1991) Modulation of neural networks for behavior, *Annu.Rev.Neurosci.*, **14**, 39–57.

[25] Hasler, M., Maistrenko, Y., and Popovych, O. (1998) Simple example of partial synchronization of chaotic systems, *Phys. Rev. E*, **58**, 6843–6846.

[26] Hasselmo, M. E., Wyble, B. P., and Wallenstein, G. V. (1996) Encoding and retrieval of episodic memories: role of cholinergic and GABAergic modulation in the hippocampus, *Hippocampus*, **6**, 693–708.

[27] Heagy, J. F., Carroll, T. L. and Pecora, L. M. (1994) Synchronous chaos in coupled oscillator systems, *Phys. Rev. E*, **50**, 1874–1885.

[28] Juergens, E., Eckhorn, R. (1997) Parallel processing by a homogeneous group of coupled model neurons can enhance, reduce and generate signal correlations, *Biological Cybernetics*, **76**, 217–227.

[29] Laurent, G. (1996) Dynamical representation of odors by oscillating and evolving neural networks, *Trends in Neurosciences*, **19**, 489–496.

[30] Maistrenko, Y., and Kapitaniak, T. (1996) Different types of chaos synchronization in two coupled piecewise linear maps, *Phys. Rev. E*, **54**, 3285–3292.

[31] Mirollo, R. E., Strogatz, S. H. (1990) Synchronization of pulse-coupled biological oscillators, *SIAM J.Appl.Math.*, **50**, 1645–1662.

[32] Murthy, V. N., Fetz, E. E. (1992) Coherent 25-30-Hz oscillations in the sensorymotor cortex of awake behaving monkeys, *PNAS*, **89**, 5670–5674.

[33] Pasemann, F. (1995) Neuromodules: A dynamical systems approach to brain modelling, in Herrmann, H., Pöppel, E., and Wolf, D. (eds.), *Supercomputing in Brain Research - From Tomography to Neural Networks*, (pp. 331–347). Singapore: World Scientific.

[34] Pasemann, F. (1995) Characteristics of periodic attractors in neural ring networks, *Neural Networks*, **8**, 421-429.

[35] Pasemann, F. (1999) Synchronized chaos and other coherent states for two coupled neurons, *Physica D*, **128**, 236–249.

[36] Pasemann, F. (1999) Synchronous and asynchronous chaos in coupled neuromodules, *International Journal of Bifurcation and Chaos*, **9**.10, to appear.

[37] Pasemann, F. (1999) Synchronized chaos in coupled neuromodules of different types, MPI-MIS Preprint 36/99, and Proceedings IJCNN'99, Washington, July 10-16, 1999.

[38] Pecora, L. M., Heagy, J. and Carroll, T. L. (1994) Synchronization and desynchronization in pulse-coupled relaxation oscillators, *Phys. Lett. A*, **186**, 225–229.

[39] Pinsky, P. F., Rinzel, J. (1994) Intrinsic and Network Rhythmogenesis in a Reduced Traub Model for CA3 Neurons, *J.Comp.Neurosci.*, **1**, 39–60.

[40] Pyragas, K. (1996) Weak and strong synchronization of chaos, *Phys. Rev. E*, **54**, R4508–4511.

[41] Roelfsma, P. R., Engel, A. K., König P., and Singer, W. (1997) Visuomotor integration is associated with zero time-lag synchronization among cortical areas, *Nature*, **385**, 157–161.

[42] Rössler, O. (1979) An equation for hyperchaos, *Phys. Lett. A*, **71**, 155–157.

[43] Schuster, H. G. (ed.) (1999) *Handbook of Chaos Control* Wiley-VCH, Weinheim.

[44] Singer, W., and Gray, C. M. (1995) Visual feature integration and the temporal correlation hypotheses, *Ann.Rev.Neuroscience*, **18**, 555–586.

[45] Skarda, C.A., and Freeman, W. (1987) How brains make chaos in order to make sense of the world. *Beh.Brain.Sci*, **10**, 161–195.

[46] Traub, R.D., Whittington, M.A., and Jeffreys, J.G.G. (1997) Gamma oscillation model predicts intensity coding by phase rather than frequency, *Neural Comp.*, **9**, 1251–1264.

[47] Treves, A. (1993) Mean-field analysis of neuronal spike dynamics, *Network*, **4**, 259–284.

[48] van Vreeswijk, C., and Sompolinsky, H. (1996) Chaos in neuronal networks with balanced excitatory and inhibitory activity, *Science*, **274**, 1724–1726.

[49] Venkataramani, S. C., Hunt, B. R., and Ott, E. (1996) Bubbling transition *Phys. Rev. E*, **54**, 1346–1360.

[50] Wang, X (1991) Period-doublings to chaos in a simple neural network: An analytic proof, *Complex Systems*, **5**, 425-441.

[51] Wang, X.J.; Buzsàki, G. (1996) Gamma Oscillation by Synaptic Inhibition in a Hippocampal Interneuronal Network Model, J. of Neurosci. 16(20), 6402–6413.

[52] Wennekers, T. and Pasemann, F. (1996) Synchronous chaos in high-dimensional modular neural networks, *Int. J. Bifurcat. Chaos*, **6**, 2055-2067.

[53] Wennekers, T. and Palm G. (1997) On the relation between neural modeling and experimental neuroscience, *Theory in Biosciences*, **116**, 273–289.

[54] Wennekers, T. and Palm G. (1999) How Imprecise is Neuronal Synchronization? *Neurocomputing*, **26-27**, 573-578.

[55] Wilson, H. R., and Cowan, J. D. (1972) Excitatory and inhibitory interactions in localized populations of model neurons, *Biophysical Journal*, **12**, 1-24.

[56] Wilson, M.A.; Bower, J.M. (1991) A Computer Simulation of Oscillatory Behavior in Primary Visual Cortex, *Neural Comp.*, **3**, 498–509.